JOURNAL OF APPLIED ELECTROCHEMISTRY **29** (1999) 371–381.

Oxidation by electrogenerated mediator: influence of perfluorosulfonic separator on process performance

S. LOGETTE[1], C. EYSSERIC[1], P. HUGUET[2], C. GAVACH[2] and G. POURCELLY[2]*

[1]*Commissariat à l'Energie Atomique, Rhône Valley Research Center, OCC/DRRV/SPHA/LEPI, Bagnols-sur-Cèze, France;* [2]*Laboratoire des Matériaux et Procédés Membranaires, CNRS, UMR 5635, 1919 Route de Mende, 34293 Montpellier Cédex 5, France*
*(*author for correspondence, e-mail: pourcell@cnrs-mop.fr)*

Received 18 December 1997; revised 12 March 1998

The electrogenerated mediator oxidation process is capable of oxidizing organic compounds to the final step, producing CO_2. It requires the use of separate compartments for the anode and cathode. A considerable electric charge is necessary to decompose long carbon chains and high-intensity electrochemical reactors are needed for use at industrial scale. A variety of porous and microporous ceramic separators (frits) have been used in industrial-scale electrochemical cells, for example, hollow cylinders made of various porous ceramics have been used to build annular cells. However, these separators exhibit a high electric resistance and one alternative is to use a perfluorosulfonic ion-exchange membrane. It is, therefore, essential to determine the flows through this membrane in order to optimize process operation. The authors describe the ion and water flows through the membrane, and their influence on the process.

Keywords: *electrogenerated mediator*, *oxidation process*, *perfluorosulfonic membrane*

1. Introduction

The electrogenerated mediator oxidation process (Fig. 1) uses a mediator to transport electrons from an anode to a substrate intended for oxidation. The mediator is a multivalent metallic ion that is reoxidized at the anode. This technology has the advantage of compatibility with low temperature (30–70 °C) operation without pressurization.

The process was originally designed to dissolve plutonium oxides, and has subsequently been developed for use with organic compounds [1–3]. It offers a promising solution for the destruction of such wastes in that it can completely oxidize most organic compounds into CO_2. The Ag(II)/Ag(I) redox pair is widely used for its strong oxidizing capacity ($E^\circ = 1.98$ V vs SHE). To obtain satisfactory oxidation performance, it is important to ensure optimum conditions for electrogeneration of the oxidizing mediator and for reaction with the substrate. This requires the use of separate compartments for the anode and cathode to prevent reducing species produced at the cathode from reacting with oxidizing species produced at the anode, diminishing the overall process yield.

A considerable electric charge is required to decompose long carbon chains such as tributylphosphate (TBP); 72 faradays are necessary to mineralize one mole of TBP. For use at industrial scale, this process therefore requires high-current electrochemical reactors. Where high currents are involved, the choice of a separator is critical. Thermal losses by the Joule effect increase with the square of the current; the very high resistance of separators such as silicon nitride implies that the power dissipation at such currents may exceed the reactor cooling capacity, resulting in unfavourable thermal conditions.

One alternative is to use an organic separator, such as an ion exchange membrane, which combines low electrical resistance with satisfactory chemical and mechanical durability. The possibility of using organic membranes with the electrogenerated mediator oxidation process was raised in the 1980s. It was shown to be a viable solution for oxidizing organic compounds although the operation of the membrane in the process has not been studied to date. Various membranes have been investigated, both ceramic and polymeric, anion or cation-exchange membranes [3–9]. In our process, a cation-exchange membrane was used. Its proton conduction property allows the protons to be transferred from the anode compartment to the cathode but not the other cations and among those, the oxidizing species Ag(II).

The membrane used in this study has, therefore, negatively charged ion sites that are equilibrated by cations. When the membrane is at equilibrium with a solution, it exhibits partial exclusion of negative charges which diminishes as the ionic strength increases.

The mediated electrolysis process operates with a nitric acid concentration exceeding 4 M. Under these

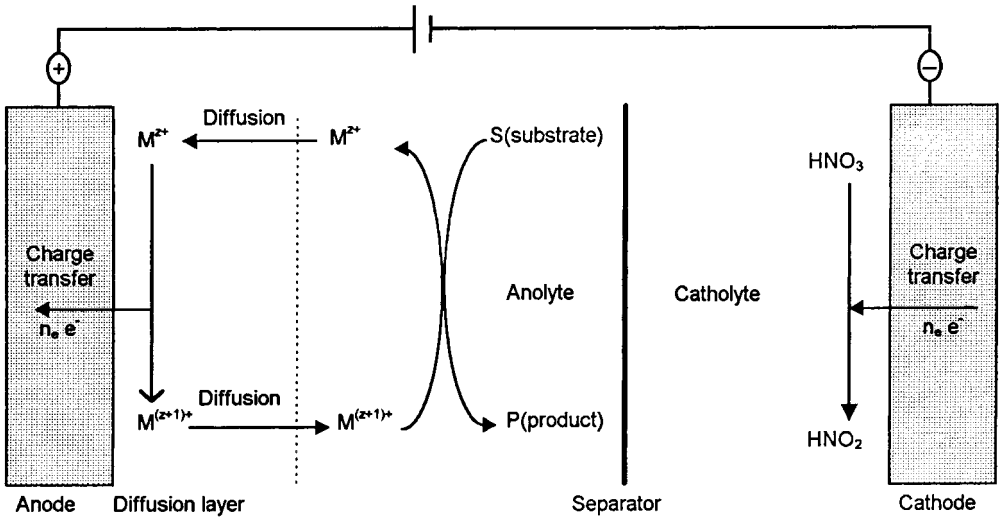

Fig. 1. Process schematic of the electrogenerated mediator oxidation.

conditions the membrane is no longer in the Donnan exclusion domain, and the electrolyte penetrates into the membrane. Free anions and cations thus exist in the interstitial solution, verifying its electroneutrality. The membrane is no longer only cation selective, the anions being involved in the transport.

The aim of this work is to understand the mechanism of ion and water transport when the membrane is at equilibrium with a concentrated electrolyte, and to study the influence of the membrane on the process performance.

2. Experimental details

2.1. *Nafion® membrane*

Measurements were made using the Nafion® 117 membrane (from Dupont de Nemours). This cation-exchange membrane was designed to be a proton conductor and its fluorinated matrix is particularly chemical resistant to oxidizing media. Its molar mass (univalent ion 1100 g equiv^{-1}) and its dry thickness (0.178 mm) were measured according to a normalized experimental protocol [10]. Its chemical resistance to oxidizing media was tested by immersing the membrane in 14 M HNO_3, 0.1 M Ag(II) or 0.1 M Ce(IV) for two months. Moreover, the Nafion® membrane immersed in 14 M HNO_3 was irradiated by a cobalt source (10^4 to 10^7 rad. integrated dose). No significant variation of exchange capacity, electrical resistance or water content was observed after these treatments.

2.2. *Electrolyte sorption*

Transport phenomena depend to a considerable extent on the membrane composition; it is therefore important to study electrolyte sorption according to the external solution concentration. The membrane is first equilibrated with a nitric acid solution, then allowed to desorb in a large quantity of water. Acid–base titration indicates the quantity of sorbed electrolyte which is then calculated per gram of dried membrane. The dried state was obtained when a constant weight of the membrane in the H^+ form was reached after it had been maintained at 60 °C under vacuum during 24 h.

2.3. *Raman spectroscopic analysis of adsorbed electrolyte*

Raman spectroscopy has already been implemented to study the membrane composition, notably to investigate the equilibrium between the two cations [11] and to identify the ionic species with sulfuric acid as the sorbed electrolyte in an anion exchange resin [12].

Raman spectra were excited with 514.5 nm radiation from an argon ion laser (Spectra Physics 2020-03) operated at about 100 mW. The spectra were recorded with an Omars 89 multichannel spectrometer (Dilor, France). The detector of our Raman spectrometer is equipped with an intensified 1024-diode array. The membrane sample was placed between two optical glasses plates that could be pressed together. Two face-to-face slots in the plates allowed Raman spectra of the membrane to be recorded without the plate material. This apparatus can be immersed in various solutions contained in an optical glass cell (Hellma). The laser beam is focused onto the edge of the sample an, at right angle to this beam, the scattered light is collected in the spectrometer. The approximate size of the probe volume is a cylinder of 50 μm of rayon and 5 mm of height. The Nafion® is a translucent sample immersed in aqueous solution, the power beam at the focal point is weak (100 mW), for these reasons, localized heating is unlikely. Pieces of Nafion® membranes were immersed in HNO_3 aqueous solutions of given composition for several days. Raman spectra of these samples were recorded between 800 and 1200 cm^{-1}, were specific bands due to nitric acid, nitrate ion and Nafion® membranes were detected. All spectra were recorded at 25 °C.

Nitric acid is characterized by two main Raman bands at 960 cm^{-1} and 1300 cm^{-1} [13]. The nitrate

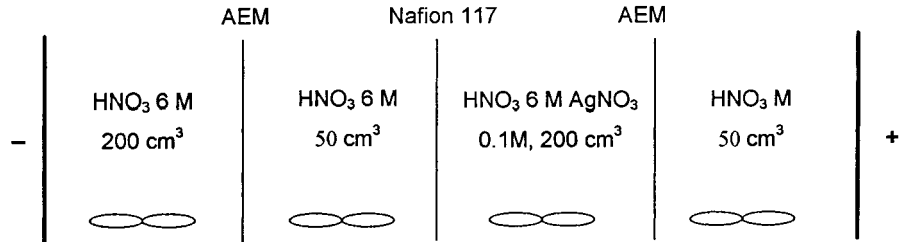

Fig. 2. Experimental setup used to measure transport numbers.

ion exhibits several Raman bands of variable intensity, with the most intense situated at 1048 cm^{-1}. Unfortunately, the Nafion® membrane possesses a band at 971 cm^{-1} corresponding to the symmetric ν_s(C–O–C) vibration, and another at 1059 cm^{-1} corresponding to SO_3^- [11]. We therefore used differential spectroscopy to monitor the HNO_3/NO_3^- ratio [14].

2.4. *Transport numbers*

Before assessing transport through the membrane, it is important to determine the composition of the sorbed electrolyte. After equilibration, the membrane was placed in a 1.5 M solution of $NaNO_3$ to desorb all the ions from the membrane. The ions were then determined by ICP–AES. Transport behaviour was then studied using a four-compartment Hittorf cell (Fig. 2) to dissociate the electrode reactions from the transport phenomena. The experiments were conducted at a current density of 100 mA cm^{-2}.

2.5. *Water transport*

Water flow conditions through the membrane constitute an important process control parameter. The flow is governed by three phenomena:

(i) *Osmosis*. This occurs in the absence of an electric field, corresponds to the passage of water molecules through the membrane when a difference in the chemical potential of the water (due to a difference in the salt concentrations) exists on either side of the membrane.
(ii) *Electroosmosis*. This corresponds to the dragging of water molecules under the effect of an electric field.
(iii) *Porosity*. This membrane may also have some small degree of porosity allowing simple Fickian diffusion.

These phenomena have been extensively investigated, but only at low concentrations (<1 M) [15] and at low current densities (0.7 A cm^{-2}) [16]. Water transport through the Nafion® 117 membrane was studied using the volume difference method with concentrated (>4 M) nitric acid to assess the effect of the current density (0.1, 0.2 and 0.3 A cm^{-2}) and the concentration (4, 6 and 12 M) on the electroosmosis flow. The cell used was already described [17]. The Nafion® 117 membrane (working area 27 cm^2) was placed between two nitric acid solutions of given composition. Calibrated glass columns were used for the variations in volume. Peristaltic pumps allowed the renewal of the solution in the two compartments with a flow rate of 6 cm s^{-1} at the solution–membrane interface.

3. Results and discussion

3.1. *Electrolyte sorption*

3.1.1. Total amount of HNO_3 sorbed. The experimental curve in Fig. 3 will subsequently be used to assess the membrane composition. The amount of sorbed electrolyte is expressed in mol of HNO_3 per gram of dried membrane n_{NO_3}/m_d.

3.1.2. Raman spectroscopic study of adsorbed electrolyte. The Nafion® 117 spectra are shown in Figs 4–7, which show the evolution of the bands according to the nitric acid concentration. The band located at 971 cm^{-1} is due to the symmetric ν_s(C–O–C) vibration, that at 1059 cm^{-1} is due to SO_3^-.

Figure 5 shows that even in dilute medium the Donnan exclusion is not complete (note the appearance of a shoulder attributable to the 1048 cm^{-1} nitrate band) but the presence of nitrates in the membrane is negligible.

The differential spectroscopy allows calculation of the ratio $n_{HNO_3}/n_{NO_3^-}(Q)$ within the membrane. The results are depicted in Fig. 8. From the ratio $n_{HNO_3}/n_{NO_3^-}$ within the membrane, the degree of

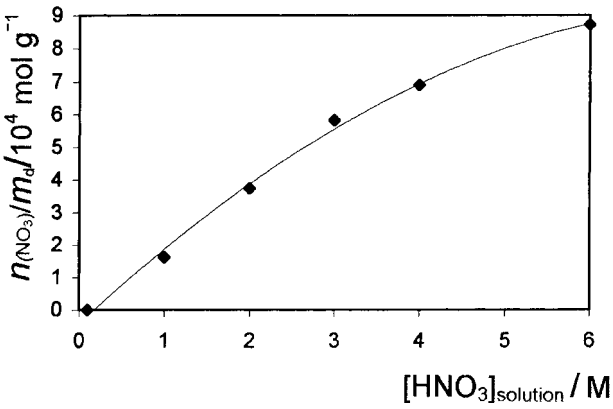

Fig. 3. Amount of sorbed HNO_3 (mol g^{-1} of dried membrane) against nitric acid concentration in solution.

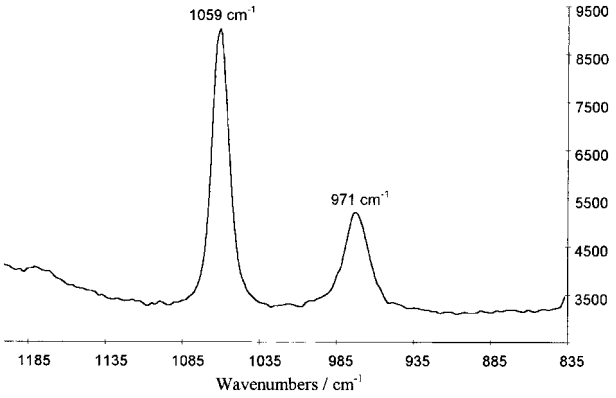

Fig. 4. Raman spectrum of Nafion® membrane equilibrated in water.

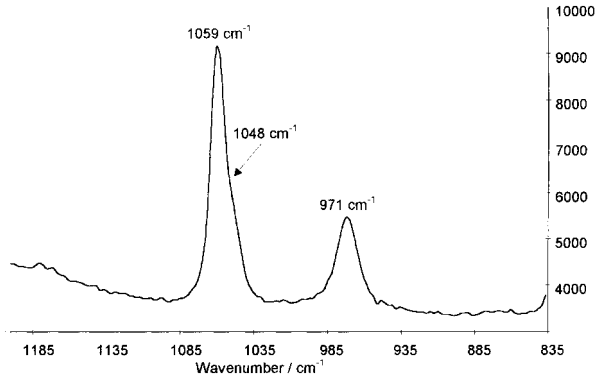

Fig. 5. Raman spectrum of Nafion® membrane equilibrated in HNO_3 (0.1 M).

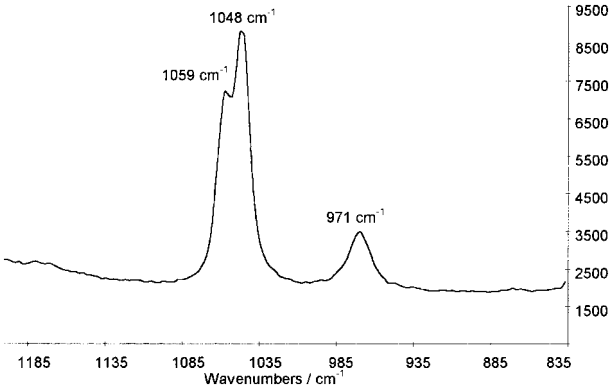

Fig. 6. Raman spectrum of Nafion® membrane equilibrated in HNO_3 (1 M).

dissociation, α, of nitric acid can be calculated from the relation $\alpha = 1/(1+Q)$.

Two conclusions may be drawn from an examination of the nature of the species sorbed according to the external concentration: (i) that molecular nitric acid is found inside the membrane at external concentrations of 7 M or higher; due to porosity; and (ii) that the ratio of molecular nitric acid to dissociated acid increases rapidly with the external concentration.

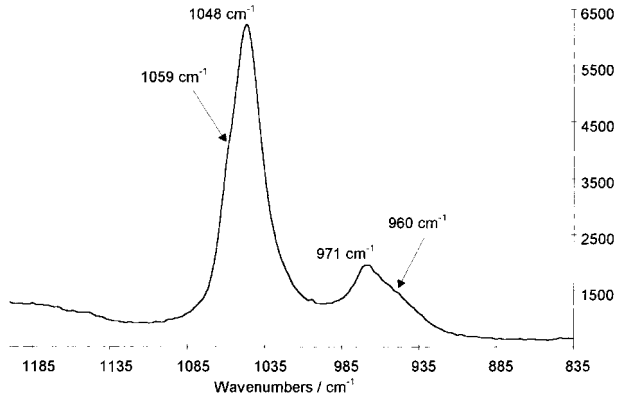

Fig. 7. Raman spectrum of Nafion® membrane equilibrated in HNO_3 (12 M).

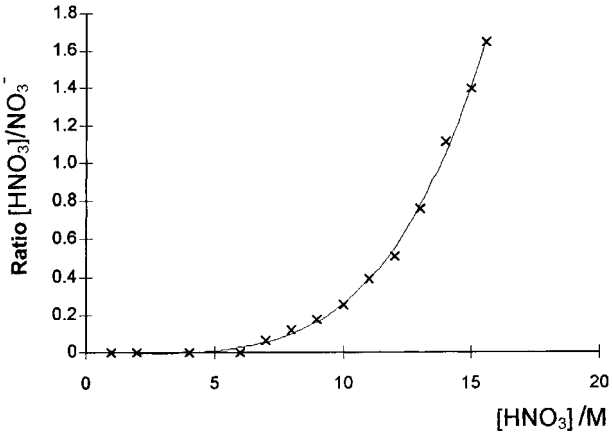

Fig. 8. Ratio of molecular nitric acid and nitrates against HNO_3 concentration in the external solution.

3.2. *Proton/cation competition in concentrated media*

3.2.1. Exchange equilibrium. To simplify the problem we had to consider two simultaneous mechanisms of transport involving the species in largest amount inside the membrane, protons, Ag^+ and nitrates. On the one hand, a *hopping mechanism* in the active region including the exchange fixed sites and the counter-ions (H^+ and Ag^+) and, on the other hand, a *dragging mechanism* in the interstitial region. The structure of the membrane is therefore accounted for according a three-phase model described in previous work [18, 19]. The hydrophobic polymer phase, the functionalized site phase (the active region) and the interstitial phase (the interstitial region). So, sulfonic exchange sites are balanced with H^+ and Ag^+ ions (amount: $\bar{n}_{H,sites}$ and $\bar{n}_{Ag,sites}$); but, the interstitial region contains the sorbed species: ($\bar{n}_{H,sorbed}$, $\bar{n}_{Ag,sorbed}$, $\bar{n}_{NO_3,sorbed}$).

The ion concentrations in the membrane are determined by assuming that the solution/membrane exchange equilibrium occurs as in dilute media, and that the sorbed electrolyte behaviour is the same as that of the external solution. The ion distribution on the membrane SO_3^- sites is calculated from the experimental curves relating the equivalent fraction in

Table 1. Ion concentrations in membrane for H^+/Ag^+ system

Aqueous solution		*Membrane*						
HNO_3 /M	$AgNO_3$ /M	$\bar{n}_{H,\,sorbed}$ /mol g^{-1}	$\bar{n}_{H,\,sites}$ /mol g^{-1}	$\bar{n}_{H,\,total}$ /mol g^{-1}	$\bar{n}_{Ag,\,sorbed}$ /mol g^{-1}	$\bar{n}_{Ag,\,sites}$ /mol g^{-1}	$\bar{n}_{Ag,\,total}$ /mol g^{-1}	$\bar{n}_{NO_3,\,sorbed}$ /mol g^{-1}
4	0.05	6.86×10^{-4}	8.99×10^{-4}	1.58×10^{-3}	8.57×10^{-6}	1.12×10^{-5}	1.98×10^{-5}	6.94×10^{-4}
	0.1	6.77×10^{-4}	8.88×10^{-4}	1.56×10^{-3}	1.69×10^{-5}	2.22×10^{-5}	3.91×10^{-5}	6.94×10^{-4}
	0.5	6.17×10^{-4}	8.09×10^{-4}	1.43×10^{-3}	7.71×10^{-5}	1.01×10^{-4}	1.78×10^{-4}	6.94×10^{-4}
6	0.05	8.69×10^{-4}	9.02×10^{-4}	1.77×10^{-3}	7.24×10^{-6}	7.52×10^{-6}	1.48×10^{-5}	8.76×10^{-4}
	0.1	8.62×10^{-4}	8.95×10^{-4}	1.76×10^{-3}	1.44×10^{-5}	1.49×10^{-5}	2.93×10^{-5}	8.76×10^{-4}
	0.5	8.09×10^{-4}	8.40×10^{-4}	1.65×10^{-3}	6.74×10^{-5}	7.00×10^{-5}	1.37×10^{-4}	8.76×10^{-4}

the membrane and in solution. The concentrations are expressed in mol g^{-1} of dry membrane.

Therefore, we have:

$$\bar{n}_{\mathrm{Ag,total}} = \bar{n}_{\mathrm{Ag,sorbed}} + \bar{n}_{\mathrm{Ag,sites}} \quad (1)$$

$$\bar{n}_{\mathrm{Ag,sorbed}} = (1 - \bar{x}_{\mathrm{H,sorbed}}) \times \bar{n}_{\mathrm{NO_3,sorbed}} \quad (2)$$

$$\bar{n}_{\mathrm{H,total}} = \bar{n}_{\mathrm{H,sorbed}} + \bar{n}_{\mathrm{H,sites}} \quad (3)$$

$$\bar{n}_{\mathrm{NO_3,total}} = \bar{n}_{\mathrm{NO_3,sorbed}} = \bar{n}_{\mathrm{H,sorbed}} + \bar{n}_{\mathrm{Ag,sorbed}} \quad (4)$$

where $\bar{x}_{\mathrm{H,sorbed}}$ is the molar fraction of protons in the interstitial region.

As shown in Table 1, the silver ions are distributed in roughly the same manner between the sorbed electrolyte and the sites (maximum difference 15%). It is thus reasonable to assume that transport occurs both via the ion sites and by the sorbed electrolyte; the difference in ion mobility between the solution and the membrane will determine which transport mechanism predominates.

The results of this model are compared with the measured values in Table 2. The precision of the experimental data is difficult to evaluate because it is not easy to know whether all the ions have been desorbed, and because the determination concerns a solution containing a few milligram per litre while the matrix contains several grams of sodium per litre. The estimated error is $\pm(5 \times 10^{-7})$ mol g^{-1}.

A satisfactory representation of the membrane composition under the process conditions can therefore be obtained by extrapolating the relative membrane/solution equilibria from the dilute medium to the concentrated and considering that the sorbed electrolyte behaves as in the external solution. This model is used for the remainder of the study.

Table 2. Experimental against theoretical results for H^+/Ag^+ system

Aqueous solution		*Membrane*	
HNO_3 /M	$AgNO_3$ /M	$\bar{n}_{Ag,\,experimental}$ /mol g^{-1} ($\pm 5\times10^{-7}$)	$\bar{n}_{Ag,\,calculated}$ /mol g^{-1}
4	0.05	1.04×10^{-5}	1.98×10^{-5}
	0.1	2.93×10^{-5}	3.91×10^{-5}
	0.5	1.62×10^{-4}	1.78×10^{-4}
6	0.05	1.24×10^{-5}	1.48×10^{-5}
	0.1	2.03×10^{-5}	2.93×10^{-5}
	0.5	8.52×10^{-5}	1.37×10^{-4}

3.2.2. Proton/cation transport competition. As for the variations of the amount of sorbed species against the external concentration, the variation of the ionic mobilities can be accounted for by the partition of the conductive part of the membrane in two regions. The transport number must be calculated strictly using the ion mobility values at the working concentration. We therefore calculated the equivalent ion conductivity of silver from the diffusion coefficient in solution reported by Farmer [20] ($D_{\mathrm{ag}} = 7.5 \times 10^{-6}$ cm^2 s^{-1}) and using the following relation developed by Nernst–Einstein (assuming this relation is still valid at these concentrations):

$$\lambda_i = \frac{F^2}{RT} z D_i \quad (5)$$

Values of equivalent ion conductivity of protons and nitrate ions (λ_{H} and $\lambda_{\mathrm{NO_3}}$) can be derived from the data of transport numbers of protons, dissociation coefficient α of nitric acids and conductivities κ of HNO_3 solutions [21], using the following relation:

$$t_{\mathrm{H}} = \frac{\alpha C_{\mathrm{H}} \lambda_{\mathrm{H}}}{\kappa} \quad (6)$$

Values of equivalent ion conductivity of protons and Ag^+ ions balancing the exchange sites of the membrane can be obtained from the values of electrical conductivities of the Nafion® membrane equilibrated with either protons or Ag^+ ions in the Donnan exclusion domain (when the membrane is equilibrated in 0.1 M HNO_3 or 0.1 M $AgNO_3$ solutions).

The values of equivalent ion conductivities of all the ionic species within the membrane are reported in Table 3. ($\lambda_{i,\mathrm{sorbed}}$ refers to the '*i*' species in the sorbed solution, $\lambda_{i,\mathrm{sites}}$ refers to the '*i*' species balancing the exchange sites).

The general expression for the transport number of a '*i*' species in the membrane is:

$$\bar{t}_i = \frac{|z_i| \bar{n}_i \lambda_i}{\sum_j |z_j| \bar{n}_j \lambda_j} \quad (7)$$

For the membrane in contact with $HNO_3 + AgNO_3$ solutions, the transport numbers for H^+, Ag^+ and NO_3^- ions are, respectively:

Table 3. Equivalent ion conductivity in 6 M nitric acid solution at infinite dilution and in membrane

Ion	$\lambda_{i,sorbed}$ /Ω^{-1} cm^{-2} eq^{-1}	λ^0 /Ω^{-1} cm^2 eq^{-1}	$\lambda_{i,sites}$ /Ω^{-1} cm^2 eq^{-1}
Ag^+	28.17	61.90	13.07
H^+	147.32	349.65	47.70
NO_3^-	44.25	71.42	–

$$\bar{t}_H = \frac{\bar{n}_{H,sorbed}\lambda_{H,sorbed} + \bar{n}_{H,sites}\lambda_{H,sites}}{W} \quad (8)$$

$$\bar{t}_{Ag} = \frac{\bar{n}_{Ag,sorbed}\lambda_{Ag,sorbed} + \bar{n}_{Ag,sites}\lambda_{Ag,sites}}{W} \quad (9)$$

$$\bar{t}_{NO_3} = \frac{\bar{n}_{NO_3,sorbed}\lambda_{NO_3,sorbed}}{W} \quad (10)$$

with

$$W = (\bar{n}_{H,sites}\lambda_{H,sites} + \bar{n}_{H,sorbed}\lambda_{H,sorbed}) + (\bar{n}_{Ag,sites}\lambda_{Ag,sites} + \bar{n}_{Ag,sorbed}\lambda_{Ag,sorbed}) + (\bar{n}_{NO_3,sorbed}\lambda_{NO_3,sorbed}) \quad (11)$$

The ion concentrations in the membrane are determined by assuming that the solution/membrane exchange equilibrium occurs as in dilute media, and that the sorbed electrolyte behaviour is the same as that of the external solution. The values of transport numbers for symmetric solutions $\{(-)[HNO_3\ 4 \text{ or } 6\,;\text{M}|\text{membrane}|HNO_3\ 4 \text{ or } 6\ \text{M} + AgNO_3](+)\}$ are collected in Table 4.

The experimental results for silver transport at 100 and 300 mA cm^{-2} indicate that the mechanism is independent on the current density; the transport from a diffusion process is negligible at such high current densities.

(a) *Asymmetric system*

The effect of implementing the process with asymmetric nitric acid concentrations was studied (with a current density of 100 mA cm^{-2}) to validate the experimental results obtained with a symmetric system (Schematic in Fig. 9).

The results obtained in symmetric and asymmetric systems are compared in Table 5. The cathodic compartment contains a 12 M HNO_3 solution for all the experiments. The values were significantly higher in the asymmetric system. This is probably attributable to the membrane/solution equilibrium. An additional experiment (Table 6) was therefore performed in a symmetric medium at 12 M to verify this hypothesis.

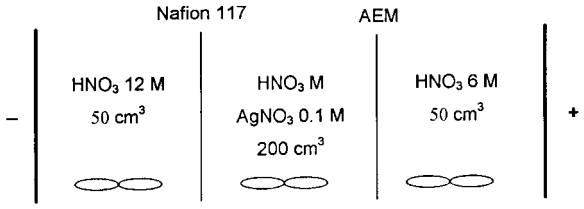

Fig. 9. Schematic of the cell for the determination of transport numbers in asymmetric systems.

The higher transport number at a concentration of 12 M can be explained by the Raman spectroscopy observations, that is, the appearance of molecular nitric acid from 7 M. Molecular nitric acid does not take part in the transport. The proton/silver ratio is thus lower than at 6 M, and the silver transport number increases.

Table 5. Transport numbers in symmetric and asymmetric systems

Aqueous solution		*Membrane*	
HNO_3 /M	*$AgNO_3$* /M	$\bar{t}_{Ag,\ asymmetric}$	$\bar{t}_{Ag,\ symmetric}$
4	0.05	6.00×10^{-3}	2.44×10^{-3}
	0.1	8.32×10^{-3}	4.80×10^{-3}
	0.5	3.46×10^{-2}	2.11×10^{-2}
6	0.05	2.31×10^{-3}	1.11×10^{-3}
	0.1	4.37×10^{-3}	2.70×10^{-3}
	0.5	1.85×10^{-2}	1.28×10^{-2}

Table 6. Effect of nitric acid concentration on silver transport through the membrane

Aqueous solution		*Membrane*
$AgNO_3$ /M	*HNO_3* /M	$\bar{t}_{Ag}$
0.1	4	4.80×10^{-3}
0.1	6	2.70×10^{-3}
0.1	12	4.68×10^{-3}

Table 4. Calculated and experimental transport numbers for H^+/Ag^+ system

Aqueous solution		*Membrane*		
HNO_3 /M	*$AgNO_3$* /M	$\bar{t}_{Ag,\ experim}$ /100 mA cm^{-2}	$\bar{t}_{Ag,\ experim}$ /300 mA cm^{-2}	$\bar{t}_{Ag,\ calc}$
4	0.05	2.44×10^{-3}	2.48×10^{-3}	1.90×10^{-3}
	0.1	4.80×10^{-3}	4.53×10^{-3}	3.79×10^{-3}
	0.5	2.11×10^{-2}	2.03×10^{-2}	1.84×10^{-2}
6	0.05	1.11×10^{-3}	1.47×10^{-3}	1.44×10^{-3}
	0.1	2.70×10^{-3}	2.99×10^{-3}	2.87×10^{-3}
	0.5	1.28×10^{-2}	1.37×10^{-2}	1.40×10^{-2}

(b) *Effect of silver concentration*
The silver(I) concentration diminishes when silver(II) is generated. The relation of the transport number t_{Ag} to the silver(I) concentration must be determined to predict the silver flow through the membrane (Fig. 10).

In the symmetric system, the transport number appears to be proportional to the silver concentration, in full agreement with the hypothesis that the silver concentration in the membrane is proportional to the concentration in solution.

In the asymmetric system, the transport number does not appear to be proportional to the silver concentration. Transport appears to be enhanced at low silver nitrate concentrations. The difficulty in this case is to understand how the membrane reaches equilibrium under dynamic conditions.

(c) *Effect of oxidant generation*
The following experiments were conducted to assess the transport of oxidized species. The experimental conditions were adjusted to ensure steady-state conditions in which electrochemical generation of the mediator was equal to its destruction by the solvent in order to ensure a constant oxidized composition.

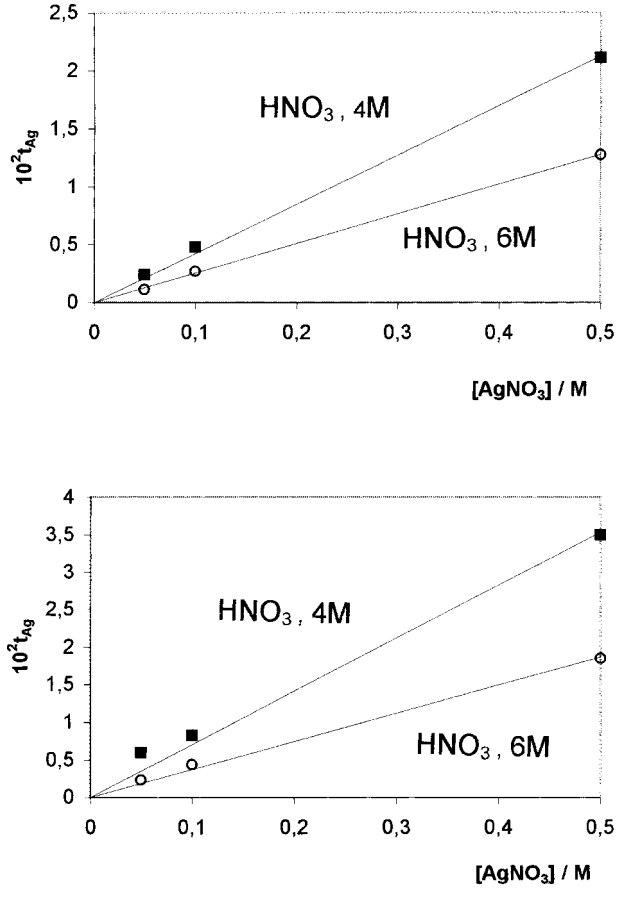

Fig. 10. Effect of silver concentration in solution on transport number in membrane. (**a**) Symmetric system; (**b**) asymmetric system.

The silver concentration was then determined on the other side of the membrane at the end of the experiment.
(i) Ag(II)/Ag(I) pair: The transport numbers obtained with and without silver(II) are compared in Table 7.

The experimental results suggest that silver(II) does not pass through the membrane; Ag(II) is found in $AgNO_3^+$ complexes, the size of which probably prevents their transport.
(ii) Effect of current density: Although the current density could be expected to have no effect on the silver transport number, experiments performed at different current densities showed significant dependence (Table 8). As the silver(II) generation curve (Fig. 11) is identical for all three current density value tested, the Ag(I)/Ag(II) ratio was the same for all three experiments.

The variation in the transport number can be explained by considering the membrane/solution equilibrium (Fig. 12).

At low current densities, the membrane equilibrium takes account of the concentrations on both sides. The transport number is therefore higher than for a symmetric system with 6 M nitric acid, since the membrane now contains molecular nitric acid. The value is also higher than for a symmetric system with 12 M nitric acid because the membrane contains proportionally more silver.

Increasing the current density induces a higher flow of species from the anolyte to the catholyte, tending to equilibrate the membrane toward a symmetric system in 6 M nitric acid.

The hydrodynamic conditions do not appear to affect the measurement. The experiment performed in a Hittorf cell at the same concentrations is fully consistent with the filter press results, as shown in Fig. 13.

3.3. *Water flow*

3.3.1. Osmosis

(a) *Experimental conditions*
Osmosis occurs in the process studied, since the nitric acid concentration varies from 4 to 6 M in the anode compartment and from 12 to 8 M in the cathode compartment. The water flow was measured over a 24-h period (Table 9); the test parameters were the nitric acid concentrations in the anolyte and catholyte.

(b) *Model*
Diffusive water flow $J_w(\mathrm{dm^3\,m^{-2}\,s^{-1}})$ through the membrane was modeled using Fick's law [21].

$$J_w = \frac{\bar{D}_w \bar{C}_w \partial \mu_w}{RT\,\partial C_w} \mathrm{grad}(C_w) \qquad (12)$$

where:

$\bar{D}_w$ water diffusion coefficient in the membrane $(\mathrm{m^2\,s^{-1}})$
$\bar{C}_w$ mean water concentration in the membrane $(\mathrm{Kg\,m^{-3}})$

Table 7. Transport with and without Ag(II)

HNO_3 /M	$AgNO_3$ /M	$\bar{t}_{Ag(I)}$ $Ag(I)$ *only*	$Ag(I)$ /*Total Ag*	$\bar{t}_{Ag(I+II)}$ $Ag(I)+Ag(II)$	$\bar{t}_{Ag(I+II)}/\bar{t}_{Ag(I)}$
4	0.05	2.44×10^{-3}	0.79	1.75×10^{-3}	0.72
	0.1	4.80×10^{-3}	0.82	3.48×10^{-3}	0.72
	0.5	2.11×10^{-2}	0.93	1.83×10^{-2}	0.87
6	0.05	1.11×10^{-3}	0.77	6.97×10^{-4}	0.62
	0.1	2.70×10^{-3}	0.72	1.66×10^{-3}	0.61
	0.5	1.28×10^{-2}	0.86	1.02×10^{-2}	0.79

Table 8. Current density against transport number

Current density /mA cm^{-2}	*Transport number* $\bar{t}_{Ag}$
65	7.0×10^{-3}
130	4.4×10^{-3}
260	3.7×10^{-3}

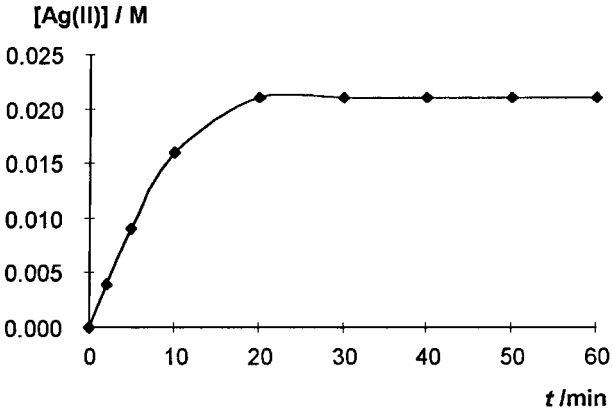

Fig. 11. Silver(II) generation at 65, 130 and 260 mA cm^{-2}.

R ideal gas constant (8.314 J mol^{-1} K^{-1})
T temperature (K)
μ_w chemical potential of water (J mol^{-1})
C_w water concentration (kg m^{-3})

The chemical potential is given by:

$$\mu_w = \mu_{ow} + RT\ln(a_w) \qquad (13)$$

where:

μ_{ow} chemical potential of water in the dilute solution (J mol^{-1})

a_w water activity

$$J = \frac{\bar{D}_w\bar{C}_w}{RT}RT\frac{\partial\ln(a_w)}{\partial C_w}\frac{\Delta C_w}{e} \qquad (14)$$

From the schematic in Fig. 14, if it is assumed that

$$\bar{C}_w = \frac{C_{w,catholyte} + C_{w,anolyte}}{2} = \frac{\Delta C_w}{2} + C_{w,catholyte} \qquad (15)$$

then

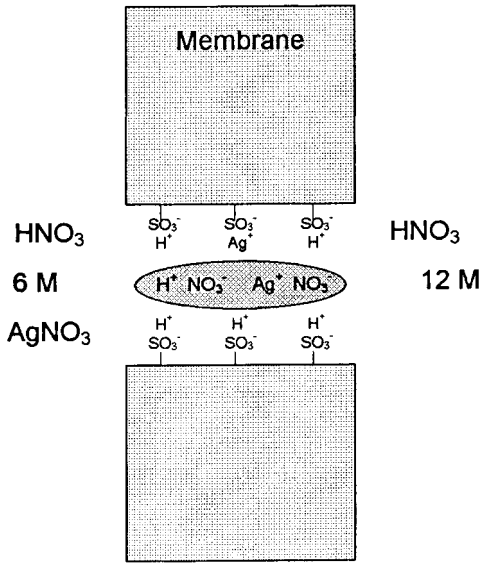

Fig. 12. Schematic representation of solution-membrane equilibrium.

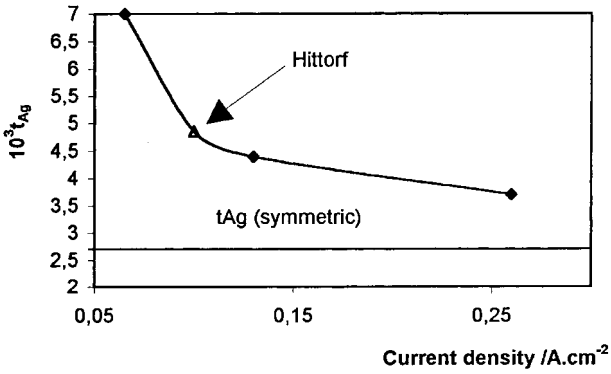

Fig. 13. Silver transport number versus current density. Symbols: (▲) Hittorf cell; (◆) filter-press cell.

Table 9. Osmotic flow ($dm^3\,m^{-2}day^{-1}$) across a Nafion®117 membrane

Catholyte [HNO_3]	Anolyte [HNO_3]		
	4 M	5 M	6 M
8 M	36.9	26.1	16.4
10 M	50.2	39.4	29.8
12 M	60.1	50.3	40.6

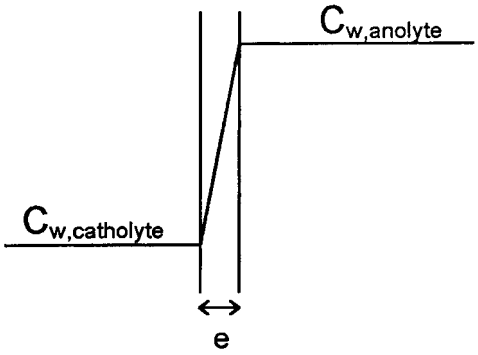

Fig. 14. Schematic representation of the water concentration profiles in the solution–membrane–solution system.

$$J_w = \frac{\bar{D}_w}{e}\frac{\partial \ln(a_w)}{\partial C_w}\left(\frac{\Delta C_w^2}{2} + C_{w,catholyte}\,\Delta C_w\right) = K\left(\frac{\Delta C_w^2}{2} + C_{w,catholyte}\Delta C_w\right) \quad (16)$$

The volume and concentration variation measurements at the end of the experiment indicate that nitric acid diffusion is negligible. The volume variation is calculated for a given Δt; the volume variation in each compartment causes the concentrations to vary:

$$\Delta V = J_w(t)S\Delta t = K\left(\frac{(C_{w,a}(t) - C_{w,c}(t))^2}{2} + C_{w,c}(t)(C_{w,a}(t) - C_{w,c}(t))\right) \times S\Delta t \quad (17a)$$

$$C_{w,c}(t+\Delta t) = \frac{C_{w,c}(t)V(t) + \frac{\Delta V d_{H_2O}}{M_{H_2O}}}{V(t) - \Delta V}$$

$$\times\ C_{w,c}(t+\Delta t) = \frac{C_{w,c}(t)V(t) + \frac{\Delta V d_{H_2O}}{M_{H_2O}}}{V(t) - \Delta V} \quad (17b)$$

$$C_{w,a}(t+\Delta t) = \frac{C_{w,a}(t)V(t) - \frac{\Delta V d_{H_2O}}{M_{H_2O}}}{V(t) - \Delta V} \quad (17c)$$

where d_{H_2O} is the density of water (10^3 kg m^{-3}).

The constant $K = -\frac{\bar{D}_w}{e}\frac{\partial \ln(a_w)}{\partial C_w}$ was determined by plotting the model curve for each experiment and minimizing the deviation $\sum(J_{exper} - J_{calc})^2$. The value of $\frac{\partial \ln(a_w)}{\partial C_w}$ was calculated as described by Davis [22], yielding a water diffusion coefficient $\bar{D}_w$ of $(2.2 \pm 0.5) \times 10^{-6}$ cm^2 s^{-1}. This value is consistent with the published value of 2.5×10^{-6}cm^2 s^{-1} at 30 °C [23].

Yeo and Eisenberg [24] investigated the effect of temperature on the diffusion coefficient, and reported an activation energy of 20.2 kJ mol^{-1}, similar to the value of 23 kJ mol^{-1} found by Morris and Sun [25]. Yeo proposes the following expression for $\bar{D}_w$:

$$\bar{D}_w = 6.0 \times 10^{-3} \exp\left(\frac{-20.2 \times 10^3}{RT}\right) \text{cm}^{-2}\,\text{s}^{-1} \quad (18)$$

3.3.2. Electroosmosis. The water transport number is a critical process control factor. The concentration in both compartments must be controlled to maintain satisfactory mediator generation characteristics and to avoid conditions resulting in hydrogen production at the cathode.

(a) *Experimental conditions*

The water transport number τ_w is defined as the number of moles of water transported per Faraday across the membrane. It is generally related to membrane properties such as the exchange capacity, the water content and structural properties, the nature and concentration of the external electrolytic solution and the current density.

The experiments were performed with identical electrolyte concentrations (4, 6, 8 and 12 M) on both sides of the membrane to avoid osmosis phenomena. Each test concentrations was studied with current intensities of 3, 6 and 12 A (i.e., current densities of 50, 100 and 200 mA cm^{-2}). The total duration of an experiment never exceeded 4 h to minimize the consequences of osmosis due to slight differences in the change of concentration in the two compartments.

The water transport number is determined experimentally by the relation:

$$\tau_w = \frac{\Delta V_c F}{M_{H_2O} I t} \quad (19)$$

where ΔV_c is the catholyte volume variation.

(b) *Discussion*

The possible formation of water by reaction at the cathode must be taken into account. The following reaction is widely accepted for the reduction of concentrated nitric acid:

$$HNO_3 + 2\,e^- + 2\,H^+ \rightarrow HNO_2 + H_2O$$

As a rough approximation, 1/2 mole of water may be assumed to form per faraday at the cathode.

The measured flows, after correction for the electrochemical production flow, indicate a transport number of 0.9 mole of water per faraday. Under symmetric operating conditions, the water transport number is independent of the concentration of the medium (4 to 12 M) and independent of the current density (50 to 200 mA cm^{-2}).

In this experiment the membrane hydration was less than 11 H_2O/SO_3H. The transport number is thus consistent with Zawodzinski's results [23]. Under identical conditions, Suzuki [26] reported a transport number of 1.1 H_2O/H^+.

(c) *Water flow and H^+ balance*

The water flow across the membrane is due to osmotic flow and to electroosmotic flow. We integrated both flows to predict the volume variations in the anode and cathode compartments. The model is

based on the diffusion model described in Section 3.3.1.(b), with the addition of the electro-osmotic flow and the reactions in solution and at the electrodes. For a given Δt, the compartment volume variations are as follows:

$$\Delta V_c = K\left(\frac{(C_{w,a}(t) - C_{w,c}(t))^2}{2} + C_{w,c}(t)(C_{w,a}(t) - C_{w,c}(t))\right) \times S\Delta t + (\tau_w + n_{w,c})M_{H_2O}\frac{I}{F}\Delta t \quad (20a)$$

$$\Delta V_a = K\left(\frac{(C_{w,a}(t) - C_{w,c}(t))^2}{2} + C_{w,c}(t)(C_{w,a}(t) - C_{w,c}(t))\right) \times S\Delta t + (\tau_w + n_{w,a})M_{H_2O}\frac{I}{F}\Delta t \quad (20b)$$

These volume variations may be used to recalculate the water concentrations in the compartments:

$$C_{w,c}(t + \Delta t) = \frac{C_{w,c}(t)V_c(t) + \frac{\Delta V_c d_{H_2O}}{M_{H_2O}}}{V_c(t) + \Delta V_c} \quad (21a)$$

$$C_{w,a}(t + \Delta t) = \frac{C_{w,a}(t)V_a(t) - \frac{\Delta V_a d_{H_2O}}{M_{H_2O}}}{V_a(t) - \Delta V_a} \quad (21b)$$

Similarly, the nitric acid concentration variation in each compartment may be calculated as follows:

$$[H]_a(t + dt) = \frac{[H]_a(t) \times V_a(t) + \frac{I}{F}\bar{t}_{NO_3}dt}{V_a(t + dt)} \quad (22a)$$

$$[H]_c(t + dt) = \frac{[H]_c(t) \times V_c(t) - \frac{I}{F}\bar{t}_{NO_3}dt}{V_c(t + dt)} \quad (22b)$$

The nitrate transport number is estimated from the studies described in Section 2. A comparison of the experimental findings with the model predictions (Table 10) is conclusive. The error percentages between the model and the experimental data for the test parameters are indicated in Table 11.

The error on the nitric acid concentration in the catholyte at the end of the experiment is attributable to several sources: the measurement error is estimated at 2.5%. The difference between the experimental and the model predictions increases with the current and can be explained by the formation of NO_x from nitrous acid, whereas the acid concentration was calculated without allowing for this transformation.

Table 11. Estimated error on parameter values

Parameter	*Max. error*
Volume variation	10%
$[HNO_3]_{anolyte}$	1.3%
$[HNO_3]_{catholyte}$	10%

Table 10. Experimental and model predictions

Experimental conditions	*Volume variation* /cm^3 h^{-1}		*$[HNO_3]_a$* /M		*$[HNO_3]_c$* /M	
	exp.	*model*	*exp.*	*model*	*exp.*	*model*
I = 2.5 A t = 1 h $[HNO_3]_a$ = 5.96 M $[HNO_3]_c$ = 12 M $[AgNO_3]_a$ = 0.096 M	8	8.6	6.0	6.1	10.7	11.6
I = 5 A t = 1 h $[HNO_3]_a$ = 5.96 M $[HNO_3]_c$ = 11.94 M $[AgNO_3]_a$ = 0.050 M	10	11	6.1	6.1	10.3	11.4
I = 5 A t = 1 h $HNO_3]_a$ = 6 M $[HNO_3]_c$ = 11.72 M $[AgNO_3]_a$ = 0.096 M	10	10.7	6.2	6.1	10.9	11.2
I = 5 A t = 1 h $HNO_3]_a$ = 6 M $[HNO_3]_c$ = 11.72 M $[AgNO_3]_a$ = 0.495 M	10	10.2	6.1	6.1	10.4	11.2
I = 10 A t = 1 h $HNO_3]_a$ = 6 M $[HNO_3]_c$ = 11.72 M $[AgNO_3]_a$ = 0.096 M	15	15.6	6.3	6.2	10.2	11.0

4. Conclusion

The optimization of the electrogenerated mediator oxidation process using a separator requires the knowledge of ion and water flows though this separator. Investigations have concerned a perflorosulfonic membrane in a nitric acid medium containing silver nitrate. They revealed the following points:

In symmetric HNO_3 systems:

(i) At the equilibrium state of the membrane sorbed nitric acid is found in dissociated form below an external nitric acid concentration of 7 M. Above 7 M, the ratio of molecular nitric acid to dissociated nitric acid increases rapidly with the external concentration.

(ii) Under electric field ion transport fluxes can be estimated as long as no molecular nitric acid is present in the membrane.

The situation is more complicated in a asymmetric system in nitric acid (4 to 6 M in the anode compartment and 12 M in the cathode compartment). Our studies showed that under these conditions the anolyte/membrane/catholyte equilibrium depends to a considerable extent on the current density, with a major increase in the silver transport number at low current densities.

The asymmetric system results in appreciable water flow by osmosis; the water diffusion coefficient determined experimentally was $2.2 \times 10^{-6}\,cm^2\,s^{-1}$. The electroosmotic flow was calculated as equal to one mole of water per transferred proton. Having determined these two flows, it will now be possible to determine changes in concentrations in the anode and cathode compartments, and thus optimize the electrolyzer operation. Finally, understanding membrane transport facilitates the design of systems for the removal and recycle of mediator from the catholyte.

References

[1] J. Bourges, C. Madic, G. Koehly and M. Lecomte, *J. Less Comm. Metals* **122** (1986) 303.

[2] J. C. Farmer, R. G. Hickman, F. T. Wang, P. R. Lewis and L. J. Summers, 'Initial study of the complete mediated electrochemcial oxidation of ethylene glycol', UCRL-LR-106479 (1991).

[3] D. F. Steele, D. Richardson, D. R. Craig, J. D. Quinn and P. Page, 'Electrochemistry for a Cleaner Environment', The Electrosynthesis Company (1992), pp. 287–300.

[4] J. C Farmer, F. T. Wang, P. R. Lewis and L. J. Summers, *Trans. Inst. Chem. Eng.* **70B** (1992) 158–64.

[5] Idem, *J. Electrochem. Soc.* **139** (1992) 3025–9.

[6] J. C. Farmer, Electrochemical treatment of mixed and hazardous wastes, *in* 'Environmental Oriented Electrochemistry' (edited by C.A.C. Sequeira), Elsevier Science Publishers B.V., Amsterdam, *The Netherlands, Studies in Environmental Science,* Series **59** (1994) 565–98.

[7] J. C. Farmer, Z. Chiba and R. G. Hickman, 'Annular-flow Electrochemical cell for Silver(II) Generation; Steady-state Performance Calculations, University of California, Lawrence Livermore National Laboratory Report UCRL-LR-106858 (1991).

[8] J. L. Ryan, L. A. Bray, E. J. Whellwright and G.H. Bryan, 'Catalyzed Electrolytic Plutonium Oxide Dissolution – The Past 17 Years and Future Potential', American Chemical Society (1992), p. 288.

[9] Z. Chiba, P. R. Lewis and R. W. Kahle, 'Mediated Electrochemical Oxidation Treatment for Rocky Flats Combustible Low-Level Mixed Waste', Annual Report: FY 1992 (1992)

[10] 'Polymeric Ion Exchange Membranes. Characterization and Test Methods of Homopolar Membranes', Norme Française NF X 45-200, AFNOR (1995).

[11] J.L. Bribes, M. El Boukari and J. Maillols, *J. Raman Spectrosc.* **22** (1991) 275.

[12] I. Tugas, J. M. Lambert, J. Maillols, J. L.Bribes, G. Pourcelly and C. Gavach, *J. Membrane Sci.* **78** (1993) 25.

[13] A. Benaouda, PhD thesis, Ecole des Mines, Paris (1995).

[14] A. Hasdou, G. Pourcelly, P. Huguet, J.L Bribes, J. Sandeaux and C. Gavach, *New J. Chem.* **20** (1996) 515–21.

[15] G. Xie and T. Okada, *J. Electrochem. Soc.* **142** (9) (1995) 3057.

[16] J. Ceynowa, *Die Angawandte Makromoleculare Chemie* **116** (1983) 165.

[17] G. Pourcelly, A. Lindheimer and C. Gavach, *J. Electroanal. Chem.* **305** (1991) 97–113.

[18] I. Tugas, G. Pourcelly and C. Gavach, *J. Membrane Sci.* **85** (1993) 183–94

[19] G. Pourcelly, I. Tugas and C. Gavach, *ibid.* **97** (1994) 99–107.

[20] J. C. Farmer, T. W. Wang, R. A. Hawley-Fedder, P. R. Lewis, J. Summers and L. Foiles, *J. Electrochem. Soc.* **139** (3) (1992) 654.

[21] A. Maurel, 'Techniques Séparatives à Membrane,' Techniques de l' Ingénieur. J2790.

[22] W. Davis and H. J. de Bruin, *J. Inorg. Nucl. Chem.* **26** (1964) 1069.

[23] T. A. Zawodzinski, C. Deruoin, S. Radzinski, R. J. Sherman, V. T. Smith, T. E. Springer and S. Gottsfeld, *J. Electrochem. Soc.* **140** (4) (1993) 1041.

[24] S. C. Yeo and A. Eisenberg, *J. Appl. Polymer. Sci.* **21** (1977) 875.

[25] D. R. Morris and X. Sun, *ibid.* **50** (1993) 1445.

[26] Y. Suzuki, M. Shibuya, F. Iwamoto, K. Suzuki, Y. Ohtou and E. Ochi, *Global 1995* **2** (1995) 1260.